Helmholtz-Zentrum Dresden-Rossendorf (HZDR)

HELMHOLTZ ZENTRUM
DRESDEN ROSSENDORF

Electronic structure studies of bismuth compounds by high energy resolution X-ray spectroscopy and ab-initio calculations

Mistonov, A. A.; Chumakov, A. P.; Ermakov, R. P.; Iskhakova, L. D.; Zakharova, A. V.; Chumakova, A. V.; Kvashnina, K. O.;

Originally published:

April 2018

Journal of Alloys and Compounds 753(2018), 646-654

DOI: https://doi.org/10.1016/j.jallcom.2018.04.190

Perma-Link to Publication Repository of HZDR:

https://www.hzdr.de/publications/Publ-26176

Release of the secondary publication
on the basis of the German Copyright Law § 38 Section 4.

CC BY-NC-ND

Electronic structure studies of bismuth compounds by high energy resolution X-ray spectroscopy and ab-initio calculations

A.A. Mistonov[1,2], A.P. Chumakov[2,3], R.P. Ermakov[4], L.D. Iskhakova[4], A.V. Zakharova[1,2], A.V. Chumakova[2], K.O. Kvashnina[5,6]

[1] *Department of Physics, Saint-Petersburg State University, 198504 Saint Petersburg, Russia*
[2] *Petersburg Nuclear Physics Institute, Gatchina, 188300 Saint Petersburg, Russia*
[3] *European Synchrotron Radiation Facility, Grenoble, France*
[4] *Fiber optic Research Center of RAS, Moscow, Russia*
[5] *Rossendorf Beamline at ESRF The European Synchrotron, CS40220, 38043 Grenoble Cedex 9, France*
[6] *Helmholtz Zentrum Dresden-Rossendorf (HZDR), Institute of Resource Ecology, P.O. Box 510119, 01314 Dresden, Germany*

(Dated: October 9, 2017)

Bismuth-based compounds are widely used as superconductors, catalysts and material for optical devices. Its properties and possibilities to control it are determined by the electronic structure and local environment of Bi-centres. Although x-ray spectroscopy is a powerful method to reveal the crystal and electronic structures, the results obtained so far were limited by the energy resolution of the experimental data. Here we report, for the first time, x-ray absorption near edge structure (XANES) data, recorded in high energy resolution fluorescence detection (HERFD) mode at the Bi L_{III} and L_I edges for the number of bismuth compounds. Experimental data are analyzed by *ab initio* calculations, using finite difference method (FDMNES) code for metallic Bi, Bi_2O_3, $BiPO_4$, $Bi_4(GeO_4)_3$ and $NaBiO_3$ compounds. It is shown, that oxidation state as well as Bi-ligand bonds length determines the exact position of the absorption edge. Additionally, the strong Bi p-d orbital mixing is observed. The obtained results can be used as an input for the further electronic structure investigations of the bismuth compounds, in different chemical states.

PACS numbers: 31.15.A- 78.70.Dm 71.20.-b 61.05.cj 78.70.En

I. INTRODUCTION

Determination of the bismuth oxidation state and local structure is problematic for series of inorganic materials: superconductors [1–5], catalysts [6–9], Bi-doped crystals [10–12], Bi-activated glasses [13–15], optical fibers [16, 17], lasers [18], amplifiers [19], superfluorescence sources [20]. Bismuth has a wide range of the oxidation states (0, +1, +2, +3, +5) and a number of polycation clusters of different charges: Bi_2^{4+}, Bi_5^{+}, Bi_5^{3+}, Bi_6^{2+}, Bi_8^{2+}, Bi_2, Bi_2^{-}, Bi_2^{2-} which can simultaneously be present in the same compound [11, 13]. Understanding not only the oxidation state, but the whole electronic structure and its relations with the crystal structure parameters allows one to determine optimal values and hence control the properties of materials produced on the base of Bi-substances. Traditionally, spectroscopic techniques are the most powerful methods for electronic structure investigation. Electrons in X-ray absorption process are excited to the first possible unoccupied level, showing the information about chemical state and interactions of the excited atom with the ligand environment.

X-ray absorption near edge structure (XANES) reflects the electronic structure of the atom in the energy range of about 30-50 eV near the absorption edge and can contain features, which are characteristic for the whole class of compounds. For instance, a chemical shift of the absorption edge is often assigned to the certain oxidation state. The position and shape of the first post edge feature is frequently used as a fingerprint of particular ligand and crystal structure environment. Because of that, analysis of new compounds requires XANES spectra of reference samples with known chemical states and structural parameters.

It was previously shown [21], that XANES spectra at Bi L_{III} absorption edge strongly depend not only on the oxidation state, but also on the local environment of Bi center. However, the energy resolution of the experimental data reported earlier [13, 15, 21–24], was not sufficient to resolve all spectral features, that prevents detailed analysis of the electronic structure. Better energy resolution of XANES spectra can be obtained by state-of-the-art experiment using high energy resolution fluorescence detection (HERFD) mode [25]. This approach allows one to resolve fine features, reflecting complexity of the electronic structure, like a pre-edge transitions, which are often not noticeable in conventional XANES experiments.

Clarity of the electronic structure is possible to achieve if theoretical approaches are exploited [26]. *Ab initio* calculations of the electronic density of states (DOS) for the absorbing atom and ligands allow to model XANES spectrum, which can be compared with the experimental results. Correspondence between experimental and theoretical spectral features link to the correctness of the used assumptions, since XANES spectrum is very sensitive to the crystal structure parameters.

In this work experimental HERFD data is recorded at the Bi L_I and L_{III} absorption edges for metallic Bi, α-Bi_2O_3, $BiPO_4$ and $Bi_4(GeO_4)_3$ and compared to the theoretical calculations using finite difference method

(FDMNES) code.

The paper is organized in the following way. Section II gives details about sample preparation, theoretical calculations and experimental setup. In Section III results and discussion are present. Section IV devoted to the concluding results.

II. SAMPLES AND METHODS

Experimental data was obtained for Bi, α-Bi_2O_3, $BiPO_4$, $Bi_4(GeO_4)_3$ and $NaBiO_3$ compounds.

Metallic bismuth and α-Bi_2O_3 were bought in Sigma Aldrich company.

$BiPO_4$ sample was synthesized at room temperature using a precipitation method. White homogeneous $BiPO_4$ precipitate was produced as a result of 0.5 bismuth nitrate water and phosphoric acid, mixed in stoichiometric relationship. Then, it was calcinated at 800°.

The monocrystalline $Bi_4(GeO_4)_3$ was grown by Czochralski process at Research Center for Laser Materials and Technologies of A. M. Prokhorov General Physics Institute, Russian Academy of Sciences.

Sodium bismuthate $NaBiO_3$ was synthesized by Aldrich Chemical Company.

The measurements were performed at beamline ID26 [27] of the European Synchrotron (ESRF) in Grenoble. The incident energy was selected using the ⟨311⟩ reflection from a double Si crystal monochromator. Rejection of higher harmonics was achieved by three Cr/Pd mirrors at an angle of 2.5 mrad relative to the incident beam. The incident X-ray beam had a flux of approximately 2×10^{13} photons/s on the sample position. XANES spectra were simultaneously measured in total fluorescence yield (TFY) mode using a photodiode and in HERFD mode using an X-ray emission spectrometer [28, 29]. The sample, five analyzer crystals and photon detector (silicon drift diode) were arranged in a vertical Rowland geometry. The Bi HERFD spectra at the L_{III} edge were obtained by recording the maximum intensity of the Bi $L_{\alpha1}$ emission line (10839 eV) as a function of the incident energy, while the Bi HERFD at the L_I edge were obtained at the maximum of the Bi $L_{\beta3}$ emission line (13211 eV). The $L_{\alpha1}$ emission energy was selected using the ⟨844⟩ reflection of four spherically bent Ge crystal analyzers (with 1 m bending radius) aligned at 82° Bragg angle and the $L_{\beta3}$ emission energy was selected using the ⟨880⟩ reflection of five spherically bent Si crystal analyzers (with 1 m bending radius) aligned at 78° Bragg angle. A combined (incident convoluted with emitted) energy resolution of 1.8 eV (2.2 eV) at the L_{III} (L_I) edge was obtained as determined by measuring the full width at half maximum (FWHM) of the elastic peak. The intensity was normalized to the incident flux.

The XANES spectra at the Bi L_I and L_{III} edges were simulated by the finite difference method for near-edge structure (FDMNES) [30].The code allows the calculation of the unoccupied projected density of states (DOS) in relation to the X-ray absorption process. Simulations were performed using an atomic clusters with 6 Åradius using Cartesian coordinates listed in the Inorganic Crystal Structure Database (ICSD) [31]. Relativistic self-consistent field calculations using the Dirac-Slater approach have been performed for each atom in the considered cluster.

III. RESULTS AND DISCUSSION

Bismuth ion has [Xe] $4f^{14}5d^{10}6s^26p^3$ ground state electron configuration and thus, depends on the oxidation state, the valence electrons are situated at the 5d, 6s and 6p orbitals. Bismuth valence 6p electrons can be probed by XANES at the Bi L_I edge, due to the dipole allowed $2s \rightarrow 6p$ transitions. While, Bi 6s and 5d electrons are probed by XANES at the L_{III} edge, due to the excitations from the $2p_{3/2}$ orbital to the empty s or d orbitals.

XANES experiment in the HERFD mode has certain advantage that the core-hole lifetime broadening, which is in order of 14.9 eV at the Bi L_I edge and 5.9 eV at the Bi L_{III} edge, can be greatly reduced, providing the high energy resolution data of the recorded XAS transitions. HERFD was performed for the number Bi systems, named Bi, Bi_2O_3, $BiPO_4$, $Bi_4(GeO_4)_3$ and $NaBiO_3$ with different oxidation states at the Bi L_I and L_{III} edges. Experimental data are shown in Fig. 1. The main difference between two absorption edges are the shape of the L_I and L_{III} edge transitions. The L_I HERFD spectra for several systems look very similar — each spectrum shows the main edge transitions (so-called “white-line”) and one or two additional features in the post-edge region. In contrast to L_I spectra the shape of the L_{III} edge spectra [Fig. 1b] differs significantly between various Bi systems. Additionally the Bi L_{III} HERFD spectra shift to higher energy upon oxidation state changes when the ligand environment remains similar. However, the energy shift is also observed when only the ligand environment or crystal structure is altered.

We analyze the electron structure by discussing first of all, the oxidation state, which is usually corresponds to the shift of the absorption edge, often determined as a first derivative maximum of the white-line. Those values of the main edge transitions at the Bi L_I and L_{III} edges are summarized in Table I, together with structural parameters of all Bi compounds.

It is clear, that for the position of the L_I edge increases with the oxidation state and most significantly for the 5+ systems, while for L_{III} the trend persist, but the position distinction is observed for non-oxidized sample.

It is well known that the energy shift of the absorption feature can be used to determine the oxidation state. For some elements and their substances the link is so univocal, that can be easily used for the revealing of the unknown oxidation state or even the mixture of them. This link arises due to 1s core-hole shielding. Potential energy of electron in an atom is determined by the attraction to

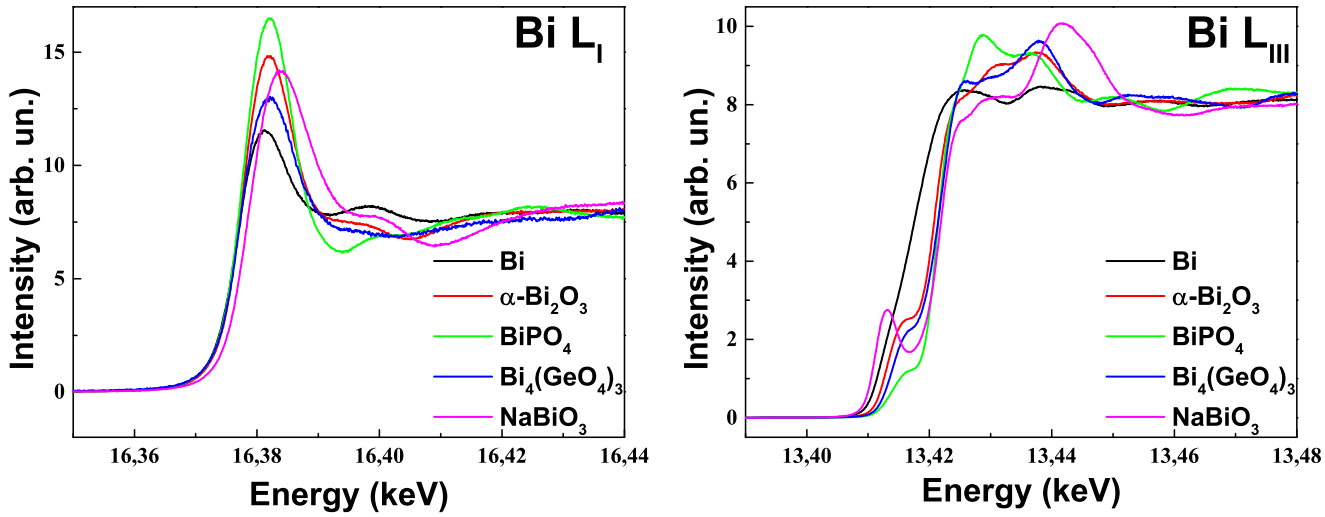

FIG. 1: (Color online) Experimental HERFD-spectra obtained at L_I (a) and L_{III} (b) edges of bismuth

positive nucleus and repulsion from the other electrons. Decreasing of electrons number (oxidation) results in lowering of the nucleus screening. The energy, needed for escape from the atom increases and absorption edge shifts towards higher energy. When the number of electrons increases, the edge shifts to lower energies [33].

However, the shift can also be due to the difference of bond length, i.e. local structure [34]. Taking it into account, theoretical calculations of the HERFD spectra was performed by considering crystal structure parameters for all Bi samples.

For example, bismuth atoms in metal are packed in $R\bar{3}m$ structure [35] and three nearest neighbours are located at distance of 3.07 Åand three next neighbours at 3.53 Å[Fig. 2a]. However, one can observe in Fig. 1 the difference in edge position for the L_{III} as it was mentioned above.

The formal oxidation state of α-Bi_2O_3,$BiPO_4$, $Bi_4(GeO_4)_3$ compounds is 3+, but structures differ considerably [Tab. I]. Bismuth oxide has two inequivalent positions. Each Bi atom with five neighbouring oxygens form strongly distorted octahedron or pyramid with slightly distorted basal plane [Fig. 2b] [36]. Bi atoms in bismuth phosphate surrounded by oxygen atoms and form a pentahedron, while phosphorus atom is in tetrahedral oxygen environment [Fig. 2c]. A single-crystal of $Bi_4(GeO_4)_3$ is an array of BiO_6 octahedra and GeO_4 tetrahedra atoms [37] [Fig. 2d].

On the other hand, the average Bi-O bond distances, are 2.329 Å [21], 2.397 Å [38] and 2.386 Å [37] for the oxide, phosphate and germanate, respectively. The bond distance will always affect on the electron density distribution. Therefore, we have a set of reference systems which are not different from this point of view. Although, the difference in crystal structure should introduce changes in the electronic structure of the Bi atom, but in case of Bi_2O_3,$BiPO_4$, $Bi_4(GeO_4)_3$ it does not influence significantly on the edge shift due to the similarity of the chemical bond distances between Bi and O. Interestingly, that $NaBiO_3$ L_{III} edge is also close to that of 3+ compounds. Its crystal structure consists of BiO_6 octahedra and NaO_6 octahedra [Fig. 2e], with the Bi-O distance of about 2.12 $\AA$ [21, 39], what is smaller than that of oxide, phosphate and germanate. Clearly, the influence of the oxidation state together with the bond length led to the shift compensation.

The shift, nevertheless, is only a preliminary indicator of the oxidation state or local environment of the absorbing atom. The most informative is the analysis of the shape and particular absorption features below and above the main edge transitions. With the aim of assigning the fine-structure components to particular electronic transitions, we performed electronic structure calculations using the FDMNES code.

Metallic Bi. Experimental and theoretical results for the metallic bismuth are reported in Fig. 3. Calculations were performed for the central Bi atom in a cluster of 26 atoms (cluster radius R = 6 Å). The main edge absorption features of L_I spectrum are due to the contribution of the p-states, while the L_{III} edge shows the main impact of the d-states. Since a metal always combines with the oxygen taken from air to form an additional product (the oxide), the additional calculations of the mixture of metallic bismuth and α-Bi_2O_3 were performed. The experimental data is better reproduced by such type of calculations for compare to the pure metallic calculations. That is, additionally, in a good agreement with x-ray diffraction data, showed the presence of 25% of oxide phase (SI.Fig.1). This addiction smooths the feature just after the white line at L_I spectrum and also slightly increases intensity of L_{III} spectrum at 13433 eV. According to our calculations a weak Bi p-d and s orbitals mixing takes place, leading to pre-edge feature, observed at the Bi L_{III} spectrum.

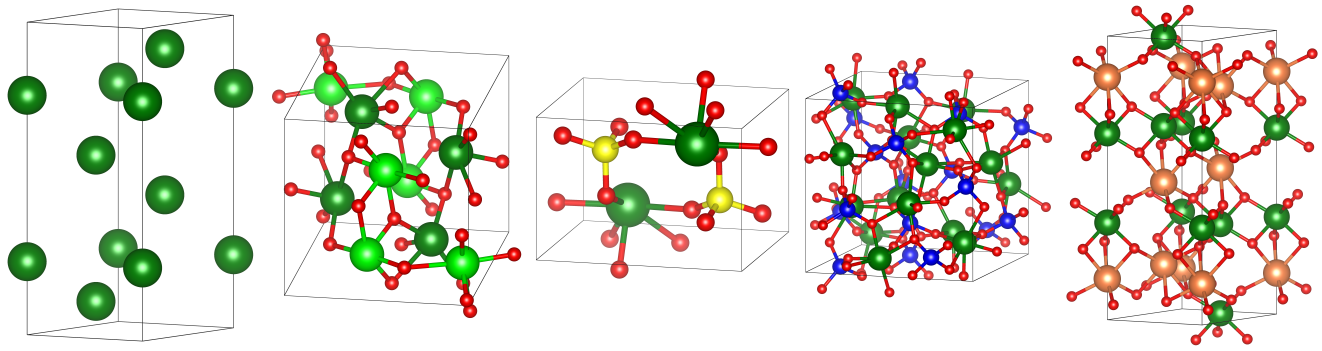

FIG. 2: (Color online) Unit cells of Bi (a), Bi_2O_3 (b), $BiPO_4$ (c), $Bi_4(GeO_4)_3$ (d) and $NaBiO_3$ (e) structures. Bismuth atoms are shown by green balls, oxygen — red, phosphorus — yellow, germanium — blue, sodium — orange

Compound	μ'_{max} **[L$_I$](eV)**	μ'_{max} **[L$_{III}$](eV)**	**Oxidation state**	**Cell parameters (Å) and angle (°)**			
				a	b	c	β
Bi [35]	16376.5	13417.3	0	4.546	4.546	11.862	90
Bi_2O_3 [36]	16377.5	13420.9	3+	5.849	8.166	7.510	113
$BiPO_4$ [38]	16377.5	13421.2	3+	4.882	7.068	4.703	96.290
$Bi_4(GeO_4)_3$ [37]	16377.1	13421.7	3+	10.524	10.524	10.524	90
$NaBiO_3$ [39]	16378.6	13421.8	5+	5.567	5.567	15.989	90

TABLE I: Positions of the L$_I$ and L$_{III}$ absorption edges and structural parameters for the studied compounds

α-Bi_2O_3. As mentioned before the metallic Bi is easily oxidized on the air. The most stable (at ambient conditions) oxide is α-Bi_2O_3. The valence 6p shell of Bi becomes completely empty at the 3+ oxidation state. The crystal structure of α-Bi_2O_3 contains two inequivalent positions of Bi atoms. The calculations, reported in Fig. 4 were performed for both Bi atoms and then averaged with respect to the number of particular atoms in the corresponded structure. The L$_I$ spectrum was calculated for the atomic cluster with radius of 5 Å(30 atoms), while L$_{III}$ spectrum — for the cluster of 6 Åradius (57 atoms). This is due to the fact that 6 Åcalculations consumed too much computer resources. Generally, the difference in cluster size may have the effect on the DOS shape and consequently on theoretical spectral features. However, this is mainly observed for the smaller cluster size (less than 3-4 Å). The L$_I$ edge experimental spectrum is very well reproduced by theoretical simulations in a cluster size of 5 Å. Existence of such strong pre-edge feature is due to mixing of p and d orbitals of Bi and p states of O.

$BiPO_4$. Figure 5 shows the experimental and theoretical data for $BiPO_4$ system. Calculations were performed for the 6 Åcluster (66 atoms). Taking into account low symmetry of the bismuth environment, one can expect strong pre-edge feature, which has been observed in calculations as well as in experimental data The phosphorus atoms are situated at 3.19 Åfrom the Bi ones and and another bismuth atoms at 4.06 Å [26, 38]. It is clear, that L$_I$-main edge features are due to p states of Bi with small admixture of Bi s, d states and O and P s and p states, while for the view of L$_{III}$ edge spectrum is strongly determined by d-states distribution. Clearly resolved peak of Bi d DOS at 13448 eV is not reflected nor theoretical nor experimental spectra. Existing of well-resolved pre-edge, mentioned above confirms p-d mixing of bismuth orbitals. It is worthy to note also, that p and s orbitals of both phosphorus and oxygen mix with ones of bismuth, giving rise to pre-edge peak and the feature near 13425 eV.

$Bi_4(GeO_4)_3$. Modelled cluster of $Bi_4(GeO_4)_3$ was of 6 Åradius and included 54 atoms. Bismuth octahedra forming the structure are distorted and inversion symmetry, thus, broken, there the p-d mixing also expected for the compound.

Fig. 6 shows, that all calculated and measured features are coincide well enough for both absorption edges, though the intensity distribution in region from 13427 eV to 13440 eV is different. Herewith, the form of Bi d DOS looks very similar to result of the experiment. Calculated spectrum reflects existence of d-f orbitals mixing. Similarly to compounds, considered above, one can note that ligands contribute significantly to beginning of the spectral range. Besides that Ge d states contribute also at the energies near 13455 eV at the L$_{III}$ edge spectrum and 16425 eV at the L$_I$ edge spectrum. Additionally, feature at the energy closed to 13440 eV is observed for all Bi compounds, where Bi is in 3+ oxidation state, shifted for $BiPO_4$ to lower energies.

$NaBiO_3$. Bi in $NaBiO_3$ compound is in his highest oxidation state (5+), meaning that not only 6p-level is empty, but 5d-level as well and dipole allowed transitions occurred at the L$_{III}$-edge differs from the ones for 3+ oxidation states.

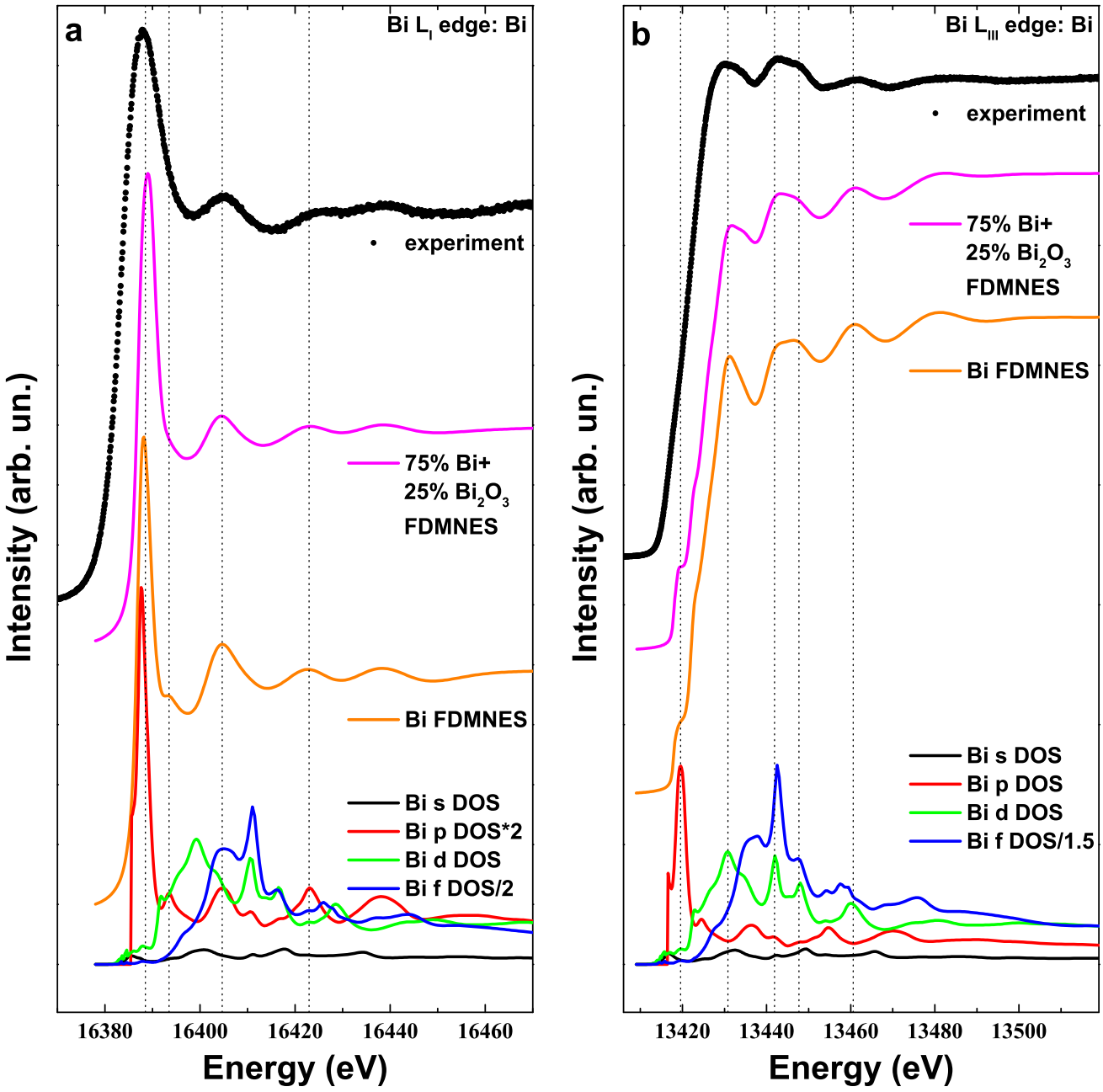

FIG. 3: (Color online) XANES spectra obtained at L_I (a) and L_{III} (b) edges for metallic Bi sample

Fig. 7 shows the experimental and calculated spectra for Bi L_I and L_{III} absorption edges. Cluster size, used for the calculations was 6 Å(57 atoms). Spectra presented in Fig. 7a are coincide well enough, while the spectra obtained at L_{III} edge are similar only at some features. The main difference is observed in pre-edge region, where strong peak clearly seen in the experimental data, while the calculated spectrum shows the evidence of two small features. This difference might arise due to the inappropriate crystal structure, which was used for the calculations. According to x-ray diffraction data (SI.Fig.2), besides the $NaBiO_3$ phase, there is an evidence of $NaBiO_3{\cdot}2H_2O$ phase formation during the synthesis. Unfortunately, there is no information about such a structure in the crystal structure database, which will allow to refine theoretical calculations. Nevertheless, the pre-edge structure in HERFD L_{III} spectra is probably due to the lowing of the symmetry of Bi environment, caused by water embedding into the structure of the main phase. Thus, the studies of $NaBiO_3{\cdot}2H_2O$ crystal structure are important for the further investigations of the electronic structure of of Bi compounds in its highest ox-

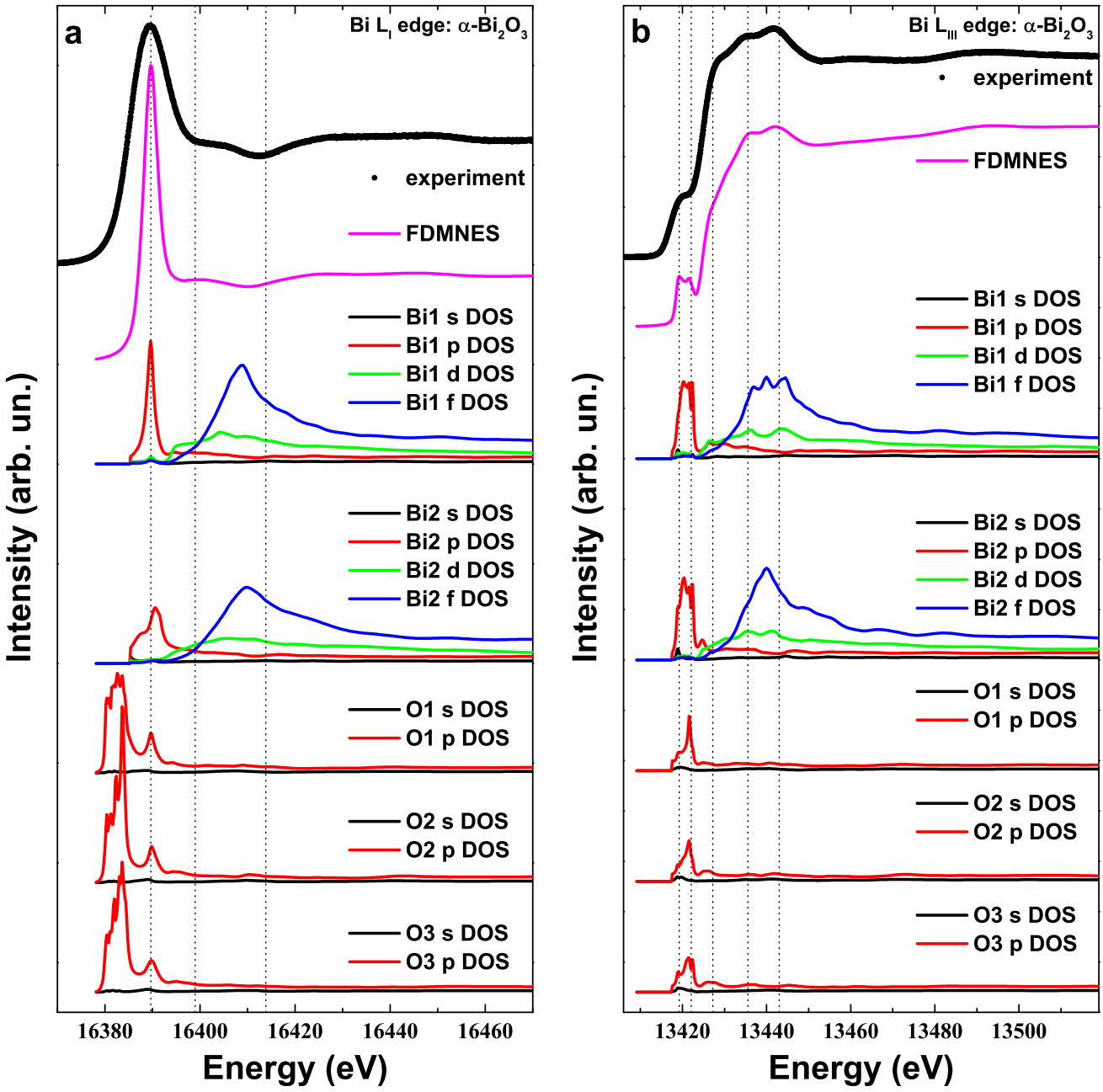

FIG. 4: (Color online) XANES spectra obtained at L_I (a) and L_{III} (b) edges for α-Bi_2O_3 sample

idation state — 5+.

Comparison between samples. Main absorption peak at the L_I edge can be assigned to 2s → 6p transition. For all the samples 6p has vacancies, but in metallic bismuth it is half-filled and hence the intensity of the main peak is the lowest. The difference in intensities for 3+ samples is obviously due to the slight difference in crystal structure. For NaBiO3 the peak amplitude decreases. Transitions observed in the spectra at the L_{III} edge for the Bi samples of 0 and 3+ oxidation states are due to the $2p_{3/2}$ → 7s and $2p_{3/2}$ → 6d excitations. According to our calculations, d DOS are major contributors, while s DOS are the minor ones, which is in agreement with previously reported work by Jiang *et al.* [21]. It was found that Bi p DOS also play significant role in the shape of the spectral transitions. Moreover, one can divide spectra of 3+ oxidation state compounds in two types depending on the stereochemical activity of Bi electron lone pair, based on the intensity and position of the white line. In this case, $BiPO_4$ belongs to one type, while α-Bi_2O_3 and $Bi_4(GeO_4)_3$ belong to another one. It is clearly seen due to the high energy resolution, that the

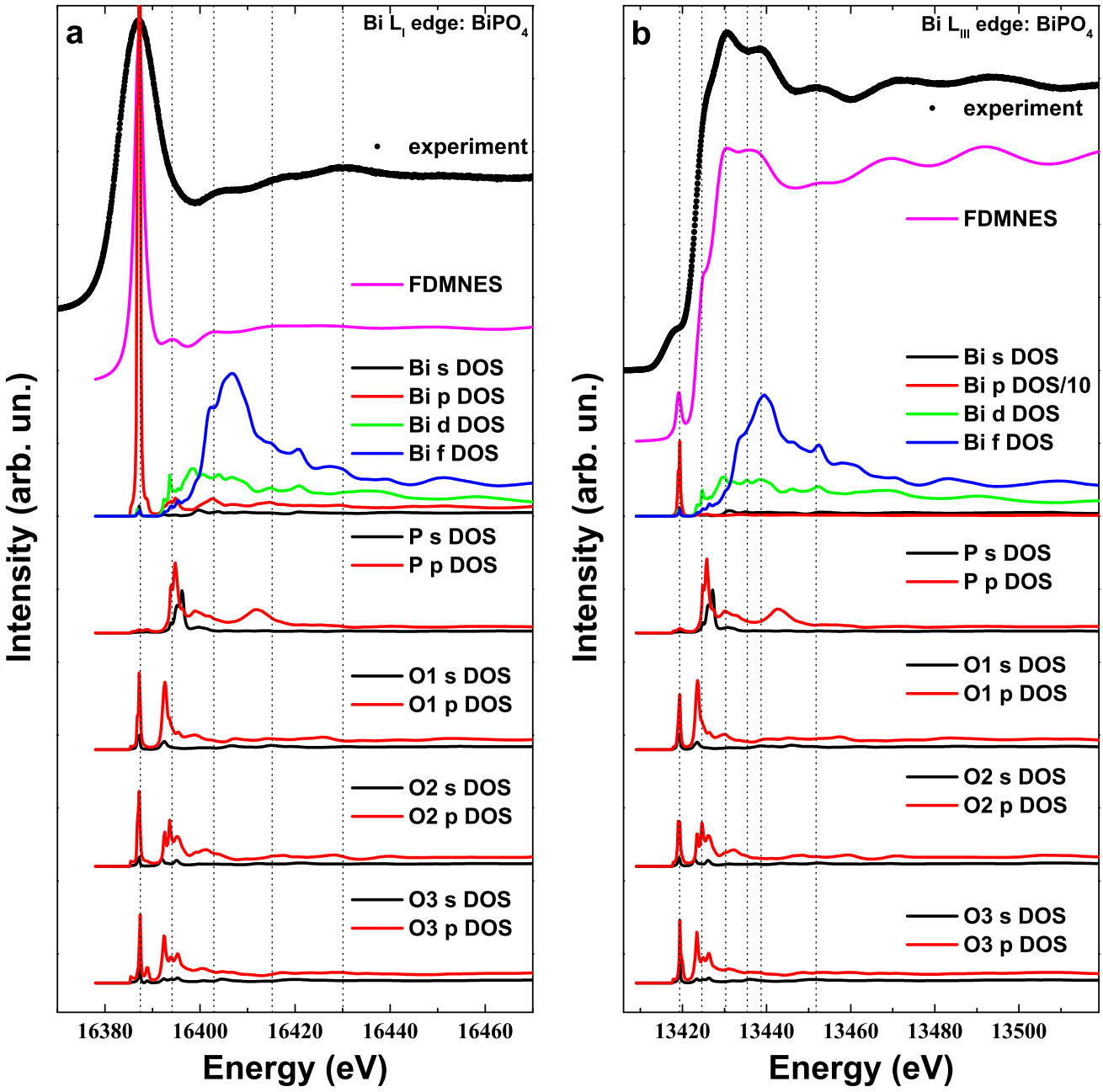

FIG. 5: (Color online) XANES spectra obtained at L_I (a) and L_{III} (b) edges for $BiPO_4$ sample

range from 13420 eV to 13440 eV contains three spectral features, positioned at 13424 eV, 13429 eV and 13440 eV. The latter has similar intensity and position for all three compounds and thus, weakly depends on the local structure or lone pair role. The main difference is observed at 13429 eV, meaning that type of environment determines significantly those transitions. One can observe strong pre-edge, produced by $2p_{3/2} \rightarrow 6p$ transition in all spectra of Bi compounds. The pre-edge structure was not observed in the experiment for metallic bismuth compound, but it should be there according to the calculations. Low intensity of that feature, detected in case of metallic Bi in comparison to other samples is due to the fact that it's p-orbital has less amount of vacancies (i.e. lower p DOS value), than others and ligands (especially oxygen) also have significant p DOS. Experimental existence of the pre-edge in case of $NaBiO_3$ can not be explained by the results of our calculations.

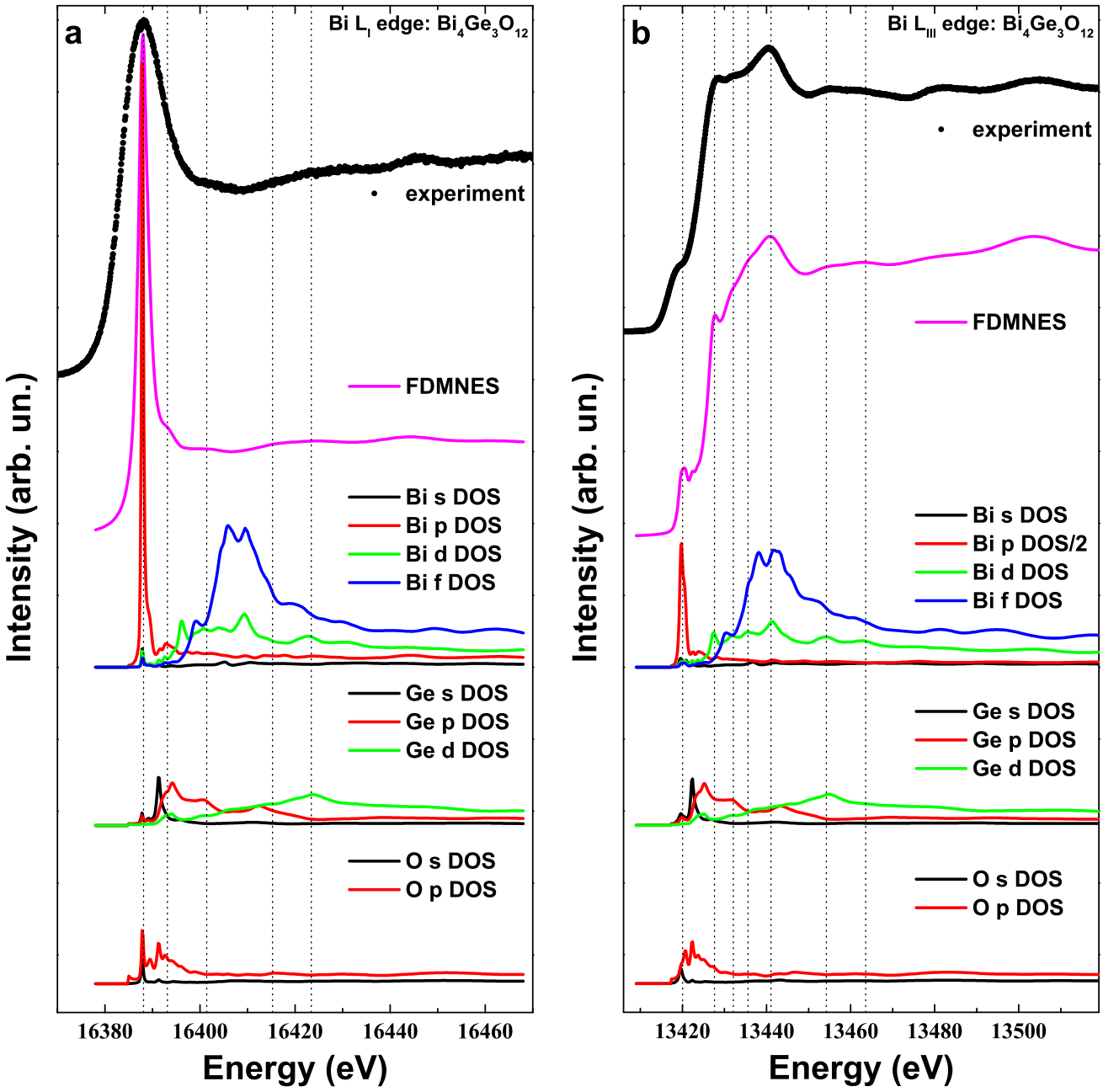

FIG. 6: (Color online) XANES spectra of $Bi_4(GeO_4)_3$ sample, obtained at L_I (a) and L_{III} (b) edges

IV. CONCLUDING REMARKS

Bi ion electronic structure in different local environment and oxidation state has been studied by HERFD spectroscopy and *ab initio* calculations. The analysis of the oxidation state changes of several Bi compounds is presented here due to its importance to understand the performance of Bi centers in several applications (e.g. superconductors and optical devices). We investigated metallic Bi, α-Bi_2O_3, $BiPO_4$, $Bi_4(GeO_4)_3$ and $NaBiO_3$ compounds.

We have shown, that the edge position is determined mostly by the Bi-O bond length. We observed, that strong p-d mixing of Bi orbitals takes place for all compounds. We have found significant contribution of the ligands like O, P and Ge to the Bi p DOS, playing the crucial role in the shape of spectrum. These results were obtained due to the high energy resolution at the synchrotron facility. It was shown also, that spectral feature at the energy about 13440 eV is specific for the 3+ oxidation state.

The are few points, which have to be considered:

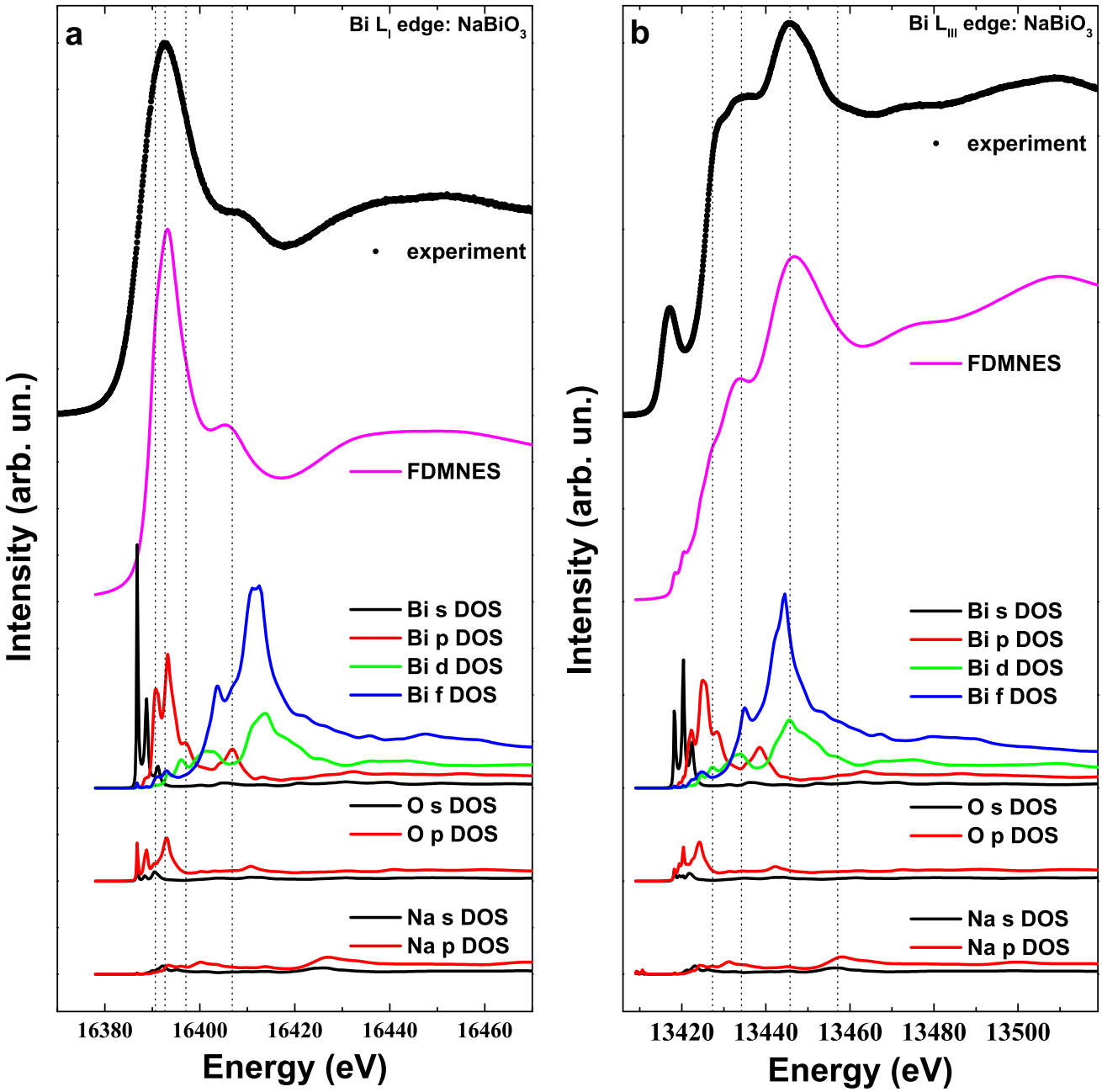

FIG. 7: (Color online) XANES spectra of $NaBiO_3$ sample at L_I (a) and L_{III} (b) edges

* Theoretical calculations have been performed for the given crystal structures, however, the errors might occur during the synthesis or due to the oxidation process of materials at the air (as in case of metalic Bi). Therefore, one needs to perform a careful characterization of each sample by X-ray diffraction or other independent methods prior HERFD experiment.

* The effect of radiation damage is also a critical issue to be considered, since reduction of Bi may also shift HERFD to low energy. We carefully studied the radiation damage issue, by collecting several fast scans (1 sec total acquisition) for the few minutes.

* HERFD is still not an unique way of assigning the oxidation state, particularly when crystal structural changes are involved. Additionally, the choice of the absorption edge plays an important role.

V. ACKNOWLEDGEMENTS

Authors acknowledge L. I. Ivleva for providing $Bi_4(GeO_4)_3$ sample and M. Sukhanov for synthesis of

$BiPO_4$ sample. Authors also would thank staff of the ID26 beamline at ESRF for the hospitality, and especially Lucia Amidani for the invaluable help during the whole experimental time.

[1] T. Wakita, E. Paris, T. Mizokawa, M.Y. Hacisalihoglu, K. Terashima, H. Okazaki, O. Proux, I. Kieffer, E. Lahera, W. Del Net, L. Olivi, Y. Takano, Y. Muraoka, T. Yokoya, N.L. Saini Determination of the local structure of $CsBi_{4-x}Pb_xTe_6$ (x = 0, 0.5) by X-ray absorption spectroscopy. // Physical Chemistry Chemical Physics 2016. - V.18. Is.36.- P.25136-25142

[2] B.J. Kim, Y.C. Kim , H.T. Kim, K.Y. Kang, J.M. Lee. EXAFS observation of two distinct Bi-O distances below Tc for a $Ba_{0.6}K_{0.4}BiO_3$ single crystal. // Physica C. 2003.- V.392-396.- P. 286-290

[3] A.N. Baranov, J.S. Kim, D.C. Kim, D.S. Suh, Y.W. Park,E.V. Antipov. X-ray absorption near-edge structure spectra study of the $Ba_{1-x}K_xBiO_3$ (0.37 ¡ x ¡ 1.0) superconductor.// Physica C. 2002. V.382. P. 95 102

[4] O. Prakash, A. Kumar, A. Thamizhavel, S. Ramakrishnan. Evidence for bulk superconductivity in pure bismuth single crystals at ambient pressure. // Science. 2017 V. 355 (6320) P.52-55. DOI: 10.1126/science.aaf8227

[5] Bismuth-based high-temperature superconductors. edited by H. Maeda and K. Togano // Applied physics (Marcel Dekker, Inc.). - New York, Basel, Hong Kong - 1996 628 PP. ISBN 0-8247-9690-X

[6] Y. Liu, G. Wang, J.C. Dong, Y. An, B. Huang, X. Qin, X. Zhang, Y. Dai A bismuth based layer structured organic-inorganic hybrid material with enhanced photo-catalytic activity // J. Colloid &Interface Science 2016 - V.469 - P.231-236

[7] Organobismuth Chemistry: Edited By H. Suzuki, Y. Matano, Elsevier, Amsterdam, The Netherlands, 2001. 636 PP. ISBN 0-444-20528-4,

[8] Bismuth-Mediated Organic Reactions, ed. T. Ollevier, Springer-Verlag, Berlin, Heidelberg, 2012; 276 PP. ISBN: 978-3-642-27238-7 (Print) 978-3-642-27239-4 (Online)

[9] T. Ollevier. New trends in bismuth-catalyzed synthetic transformations. // Org. Biomol. Chem. 2013. V. 11 P.2740-2755. DOI: 10.1039/C3OB26537D

[10] M. de Jong, A. Meijerink, R.A. Gordon, Z. Barandiara, L. Seijo Is Bi^{2+} Responsible for the Red-Orange Emission of Bismuth-Doped SrB_4O_7?//J. Phys. Chem. 2014, V.118. P. 9696-9705

[11] H.T. San, J. Zhou, J. Qui Recent advances in bismuth activated photonic materials.//Progress in Mat. Sci. 2014.- V.64. - P.1-72

[12] V. Carceln, P. Hidalgo, J. Rodrguez-Fernndez, E. Dieguez. Growth of Bi doped cadmium zinc telluride single crystals by Bridgman oscillation method and its structural, optical, and electrical analyses. // Org. Biomol. Chem. 2010 V. 107(9) P. 093501-093501-4. DOI: http://dx.doi.org/10.1063/1.3275054

[13] X. Jiang, L. Su, P. Yu, X. Guo, H. Tang, X. Xu, L. Zheng, H. Li, J. Xu Broadband photolu-minescence of Bi_2O_3 GeO_2 binary systems: glass, glass-ceramics and crystals // Laser Phys. 2013. V.23. - P.105812

[14] I. Manzini, P.P. Lottici, G. Antonioli. EXAFS at the Bi L_{III} edge in $Bi_4Ge_4O_{12}$ and in xBi2O3 (100-x) GeO2 glasses. // J. Non-Cryst. Solids. 1998.- V.224. P. 23-30

[15] A. Witkowska, J. Rybicki, A. Di Cicco. Structure of partially reduced bismuthsilicate glasses: EXAFS and MD study// J. Alloys&Comp. 2005. V. 401. - P.135-144

[16] E.M. Dianov. Amplification in Extended Transmission Bands Using Bismuth-Doped Optical Fibers.// J. Lightwave Techn. 2013. - V.31. Is.4. - P.681-688.

[17] L.D. Iskhakova, F.O. Milovich, V.M. Mashinsky, A.S. Zlenko, S.E. Borisovsky, E.M. Dianov Identification of Nanocrystalline Inclusions in Bismuth-Doped Silica Fibers and Preforms.// Microscopy and Microanalysis, V. 22, Is. 5, pp. 987-996

[18] I.A. Bufetov, E.M. Dianov Bi-doped fiber lasers.// Laser Physics Lett. 2009. 6, P.487-504.

[19] E.M. Dianov Bismuth-doped optical fibers: a challenging active medium for near-IR lasers and optical amplifiers// Light: Science&Applications 2012. V.1. P.e12-e18.

[20] K.E. Riumkin, M.A. Melkumov, I.A. Bufetov, A.V. Shubin, Firstov, S.V.V.F. Khopin, A.N Guryanov, E.M Dianov Superfluorescent 1.44 mu m bismuth-doped fiber source // Optics letters. 2012. V.37. Is. 23. PP. 4817-4819

[21] N. Jiang, J.C.H. Spence Can near-edge structure of the Bi L_3 edge determine the formal valence states of Bi?// J. Phys.: Condens. Matter 2006. V.18. P.80298036

[22] B. Tooth, B. Etschmann, G. S. Pokrovski, D. Testemale, J.-L. Hazemann, P. V. Grundler, J. Brugger. Bismuth speciation in hydrothermal fluids: An X-ray absorption spectroscopy and solubility study. // Geochimica et Cosmochimica Acta. 2013 V. 101 P.156-172.

[23] A. Corrias, L. Pincombe, G. Mountjoy, V.M. Mashinsky, A.S. Zlenko, N.M. Karatun, B.I. Denker, S.E. Sverchkov, B.I. Galagan, A.A. Umnikov, A.N. Guryanov, E.M. Dianov, S. Di-az-Moreno A Bi L_3-edge X-Ray Absorption Spectroscopy Study of the Role of Bi in Bi-doped Glasses for Fibre Lasers// 13^{th} Int. Conference on the Structure of Non-Crystalline Materials. 2016. Canada, July 24-29. P.32

[24] B.J. Kim, Y.C. Kim , H.-T. Kim, K.-Y. Kang, J.M. Lee. EXAFS observation of two distinct Bi-O distances below Tc for a $Ba_{0.6}K_{0.4}BiO_3$ single crystal.//Physica C. 2003. V.392-396. P. 286-290

[25] S.M. Butorin, K.O. Kvashnina, J.R. Vegeliusa, D. Meyerd, D.K. Shuhe. High-resolution X-ray absorption spectroscopy as a probe of crystal-field and covalency effects in actinide compounds//Proc. NAS USA2016. - V. 113. Is.23 - P.8093-8097

[26] A. Walsh, G.W. Watson, D.J. Payne, R.G. Edgell, J. Guo, P.-A. Glans, T. Learmonth, K. Smith. Electronic structure of the α and δ phases of Bi_2O_3: A combined ab initio and x-ray spectroscopy study.// Phys. Rev. B. 2006. - V.73 (23) - P. 235104-235117.

[27] C. Gauthier, V.A. Sole, R. Signorato, J. Goulon, E. Moguiline The ESRF beamline ID26: X-ray absorption on ultra dilute sample// J. Synchrotron Rad. 1999. V.6. P. 164-166

[28] P. Glatzel, U. Bergmann, Coord. Chem. Rev. 2005, 249, 6595.

[29] K. O. Kvashnina, A. C. Scheinost, J. Synchrotron Radiat. 2016, 23, 836841.
[30] Y.Joly. X-ray absorption near-edge structure calculations beyond the muffin-tin approximation.// Phys.Rev.B. 2001 - V.63 - P. 125120 -125130.
[31] https://icsd.fiz-karlsruhe.de/search/index.xhtml
[32] Etschmann et al., Chemical Geology, 425, 37-51 (2016)
[33] Eisenberger P, Kincaid BM (1978) EXAFS: new horizons in structure determinations. Science 200:14411447
[34] Bunker G., Introduction to XAFS. A practical guide to x-ray absorption fine structure spectroscopy, Cambridge University Press, 2010
[35] P.Cucka, C. S. Barrett.The crystal structure of Bi and of solid solutions of Pb, Sn, Sb and Te in Bi.//Acta Crystallographica. 1962 - V.15 (9) - P. 865-872.
[36] G. Malmros. The crystal structure of alpha - Bi2O3.// Acta Chemica Scandinavica. 1970 - V. 24 - P. 384-396.
[37] S.F. Radaev, L.A. Muradyan, Yu.F. Kargin, V.A. Sarin, V.N. Kanepit, V.I. Simonov.Neutron diffraction study of single crystals of Bi4Ge3O12 with eulitine structure.// Kristallografiya. 1990 - V. 35 - P. 361-364
[38] S.N. Achary, D. Errandonea, A. Muoz,P. Rodrguez-Hernndez,F.J. Manjn,P.S. Krishna,S.J.Patwe, V. Grover, A.K. Tyagi.Experimental and theoretical investigations on the polymorphism and metastability of BiPO4.// Dalton Trans. 2013. - V. 14(42) - P. 14999-5015.
[39] N.Kumada, N. Kinomura, A.W. Sleight. Neutron powder diffraction refinement of ilmenite-type bismuth oxides: ABiO3 (A = Na, Ag).// Materials Research Bulletin. 2000 - V.35 - P.2397-2402.